Asian Journal of Andrology (2011) 13, 481–486

www.nature.com/aja

ORIGINAL ARTICLE

Plasmid-based *Stat3* siRNA delivered by hydroxyapatite nanoparticles suppresses mouse prostate tumour growth *in vivo*

Zuo-Wen Liang[1,*], Bao-Feng Guo[2,*], Yang Li[1], Xiao-Jie Li[1], Xin Li[1], Li-Jing Zhao[1], Li-Fang Gao[1], Hao Yu[1], Xue-Jian Zhao[1], Ling Zhang[1] and Bao-Xue Yang[3]

DNA vector-based *Stat3*-specific RNA interference (si-*Stat3*) blocks *Stat3* signalling and inhibits prostate tumour growth. However, the antitumour activity depends on the efficient delivery of si-*Stat3*. The effects on the growth of mouse prostate cancer cells of si-*Stat3* delivered by hydroxyapatite were determined in this study. RM-1 tumour blocks were transplanted into C57BL/6 mice. $CaCl_2$-modified hydroxyapatite carrying si-*Stat3* plasmids were injected into tumours, and tumour growth and histology were determined. The expression levels of *Stat3*, *pTyr-Stat3*, *Bcl-2*, *Bax*, *Caspase3*, *VEGF* and *cyclin D1* were measured by western blot analysis. Amounts of apoptosis in cancer cells were analysed with immunohistochemistry and the terminal deoxyribonucleotidyl transferase-mediated dUTP-digoxigenin nick end-labelling (TUNEL) assay. The results showed that hydroxyapatite-delivered si-*Stat3* significantly suppressed tumour growth up to 74% ($P<0.01$). *Stat3* expression was dramatically downregulated in the tumours. The immunohistochemistry and TUNEL results showed that si-*Stat3*-induced apoptosis (up to 42%, $P<0.01$). The *Stat3* downstream genes *Bcl-2*, *VEGF* and *cyclin D1* were also strongly downregulated in the tumour tissues that also displayed significant increases in *Bax* expression and Caspase3 activity. These results suggest that hydroxyapatite can be used for the *in vivo* delivery of plasmid-based siRNAs into tumours.

Asian Journal of Andrology (2011) **13,** 481–486; doi:10.1038/aja.2010.167; published online 7 February 2011

Keywords: apoptosis; hydroxyapatite; prostate cancer; RNA interference; *Stat3*

INTRODUCTION

RNA interference (RNAi) is a method of post-transcriptional gene silencing. Small interfering RNAs (siRNAs) can be chemically synthesised or expressed from a DNA vector.[1,2] Recently, RNAi has been recognized as a novel and promising antitumour strategy.[3] However, one of the challenges of the *in vivo* application of siRNA-based therapies is the efficient delivery of siRNA, especially across the plasma membrane, to the cytoplasm of target cells.

Nanomedicine is a newly emerging practice that fuses nanotechnology and medicine. Nanoparticles have been used as diagnostic probes in targeted therapy. Hydroxyapatite (HAP) is the principal inorganic constituent of human bones and teeth, and its molecular formula is $Ca_{10}(PO_4)_6(OH)_2$.[4] Synthetic HAP crystals are now widely used in medical implants and as coatings on prostheses.[5] Compared to viral vectors, which possess risks of pathogenicity and immunogenicity, synthetic HAP nanoparticles have favourable biocompatibility and high osteoconductivity and/or osteoinductivity without immunogenicity or proinflammatory features.[6–9] HAP can not only directly inhibit the proliferation of cancer cells,[10] but also be used in a gene delivery system due to its safety, economy and efficiency.[11]

Our previous study showed that *Stat3*-specific siRNA can markedly suppress *Stat3* expression and inhibit the growth of prostate cancer cells.[12] In this study, HAP nanoparticles were used to mediate DNA vector-based *Stat3*-specific RNAi to treat prostate cancer *in vivo*, with the goal of investigating the *in vivo* antitumour efficacy of HAP nanoparticle-mediated RNAi.

MATERIALS AND METHODS

HAP and *Stat3*-specific siRNA plasmids

HAP nanoparticles were purchased from Nanjing Emperor Nano Material Co. Ltd (Nanjing, China). Expression plasmids containing *Stat3*-specific siRNA were constructed in our laboratory. According to our previous study, the si-*Stat3* most effective at inhibiting cancer growth is located at the SH2 domain of the mouse and human *Stat3* genes.[12] Thus, this si-*Stat3* (sequence: GCAGCAGCTGAACAACA-TG, spanning nucleotides 2144 to 2162; GenBank accession number: NM_003150) was used in the present study. A negative control si-scramble sequence (Ambion, Austin, TX, USA) without obvious homology to mouse or human gene sequences was used to eliminate nonspecific effects. HAP was ultrasonically processed for 10 min, and

[1]Prostate Diseases Prevention and Treatment Research Centre and Department of Pathophysiology, Norman Bethune Medical School, Jilin University, Changchun 130021, China; [2]Department of Emergency Medicine, China–Japan Union Hospital of Jilin University, Changchun 130033, China and [3]Department of Pharmacology, School of Basic Medical Sciences, Peking University, Beijing 100191, China

* These authors contributed equally to this work.

Correspondence: Professor Ling Zhang (zhangling3@jlu.edu.cn) or Professor Bao-Xue Yang (baoxue@bjmu.edu.cn)

Received: 2 September 2010; Revised: 3 November 2010; Accepted: 9 November 2010; Published online: 7 February 2011

the final concentration was adjusted to 20 μg μl^{-1}. A $CaCl_2$ solution was prepared with double-distilled water at a final concentration of 0.25 mol l^{-1}. Then, 20 μl of HAP and 25 μl of $CaCl_2$ were gently mixed by repeated inversion and ultrasonically processed for 10 min. Subsequently, 20 μg (40 μl, 0.5 μg μl^{-1}) of plasmid was added to the above solution, producing a final volume of 100 μl. This solution was incubated for 20 min at room temperature and mixed by repeated inversion before injection.

Cell culture and establishment of a mouse prostate cancer model

The mouse prostate cancer cell line RM-1 was obtained from the Shanghai Institute of Cellular Research (Shanghai, China). These cells were grown in Iscove's modified Dulbecco's medium (GIBCO, Carlsbad, CA, USA) containing 10% foetal bovine serum (GIBCO). Then, RM-1 cells (2×10^6 cells per 150 μl) were transplanted into mice subcutaneously to generate a primary cancer. Male C57BL/6 mice, weighing 18–22 g, were purchased from the Beijing Institute for Experimental Animals (Beijing, China). All animals were housed and experiments were performed according to the guidelines established by Jilin University for the ethical use of animals in research. The tumours were obtained, cut into 1.5-mm^3 blocks and implanted into the right flanks of C57BL/6 mice. Five days after implantation, the mice were divided into three groups (n=8 per group) and independently injected intravenously with 100 μl of (i) phosphate-buffered saline (PBS) alone (mock), (ii) $CaCl_2$-modified HAP carrying p*Silencer*^{neo} 3.1-H1-Scrambled siRNA (HAP-si-Scramble; control), or (iii) $CaCl_2$-modified HAP carrying p*Silencer*^{neo} 3.1-H1-*Stat3*-siRNA (HAP-si-*Stat3*). $CaCl_2$-modified HAP carrying plasmids (20 μg per mouse) were subcutaneously injected into the tumours at different sites using a syringe with a 27-gauge needle. The tumour volume was calculated approximately every 2 to 3 days according to the following formula: $m_1\times m_2\times0.5236$ (m_1: short diameter; m_2: long diameter).[13] This process was repeated on day 20. The mice were killed on day 32, and the tumours from the different groups were obtained for immunohistochemistry and terminal deoxyribonucleotidyl transferase-mediated dUTP-digoxigenin nick end-labelling (TUNEL) assays.

Semiquantitative reverse transcription-PCR (RT-PCR)

The mRNA expression levels of *Stat3* and the *Stat3* downstream genes were determined using semiquantitative RT-PCR. Total RNA was isolated from tumours using TRIzol (Invitrogen, Carlsbad, CA, USA) according to the manufacturer's instructions. Reverse transcription was performed with 3 μg of total RNA in a final volume of 20 μl containing 10 mmol l^{-1} dNTP, 0.5 μg μl^{-1} oligo dT, 20 U RNasin and 200 U M-MLV reverse transcriptase (Promega Corp., Madison, WI, USA). PCR was performed in a final volume of 25 μl containing 25 mmol l^{-1} $MgCl_2$, 2.5 mmol l^{-1} dNTP and 1 U Taq DNA polymerase (Invitrogen). The sequence of the PCR primers (Sangong Co. Ltd, Shanghai, China) was based on the mouse mRNA. The PCR products were separated by 1% agarose gel electrophoresis and visualised under UV light after 0.5% ethidium bromide staining. The primers specific to the candidate genes were designed using Primer 5 software (PREMIER Biosoft International, Palo Alto, CA, USA). The primer sequences were as follows: *GAPDH* sense, 5′-GGGTGATGCTGGTGCTGAGTATGT-3′ and antisense, 5′-AAGAATGGGAGTTGCTGTTGAAGTC-3′; *Stat3* sense, 5′-TTGCCAGTTGTGGTGATC-3′ and antisense, 5′AGAACCCAGA-AGGAGAAGC-3′.

Western blot assay

Cell lysis, protein quantifications and Western blot assays were performed as previously described.[14] The anti-Stat3, anti-phospho-Tyr705-Stat3, anti-cyclin D1, anti-VEGF and anti-β-actin antibodies were obtained from Santa Cruz Biotech, Inc. (Santa Cruz, CA, USA). The anti-Bcl-2, anti-Bax and anti-cleaved-caspase3 antibodies were obtained from Cell Signalling Technology (Beverly, MA, USA). The protein bands were visualised by SuperSignal West Pico Chemiluminescent Substrate (Pierce, Rockford, IL, USA), and the membranes were subjected to X-ray autoradiography. Band intensities were determined with Quantity One software (Bio-Rad). Experiments were performed in triplicate, and the results were expressed as means±s.e.

Immunohistochemistry and TUNEL assay

Serial sections of tumour tissue excised from animals were fixed in formalin. Immunostaining was performed using the Vectastain Elite ABC avidin/biotin staining kit (Vector Laboratories Inc., Burlingame, CA, USA). Antibodies specific to Stat3, proliferating cell nuclear antigen (PCNA) and CD34 were obtained from Santa Cruz Biotech, Inc. The DeadEnd Fluorometric TUNEL System (Promega) was used to measure the fragmented DNA in apoptotic cells by catalytically incorporating fluorescein-12-dUTP at the 3′-OH DNA ends using terminal deoxynucleotidyl transferase, recombinant (rTdT) (Promega). Paraffin-embedded tissues were cut into 3-μm sections, deparaffinised and hydrated according to standard protocols.[15] After incubation with proteinase K (20 μg ml^{-1}) for 30 min at room temperature, the TUNEL reaction mix containing rTdT and the rTdT reaction mix was added to the slides, followed by incubation in a humidified chamber for 60 s at 37 °C. After being washed, the sections were immersed in 40 ml of freshly prepared propidium iodide solution (1 μg ml^{-1}) for 15 min at room temperature in the dark. The reaction was visualised by a laser scanning confocal microscope. TUNEL-positive cells exhibited green fluorescence.

Statistical analysis

Quantitative data were expressed as mean±SE. Statistical analysis was performed with SPSS version 13.0 (SPSS Inc., Chicago, IL, USA), and one-way ANOVA was used to compare the differences between groups. $P<0.05$ was considered statistically significant.

RESULTS

Antitumour activity of si-*Stat3*

To evaluate the effects of HAP-mediated si-*Stat3* transfection on the growth of prostate cancer *in vivo*, the antitumour efficacy was determined using a prostate cancer RM-1 mouse model. Primary tumour blocks (1.5 mm^3) were implanted into the right abdomens of C57BL/6 mice as previously described.[16] On day 5, tumours were visible at the sites of implantation (mean volume: 52.7±12.1 mm^3, n=8). Cancer bearing mice were independently injected intratumourally with PBS, HAP-si-scramble or HAP-si-*Stat3*, which was repeated on day 20. The animals were killed on day 32, and the tumour sizes were measured (Table 1). A significant difference in tumour size was found between the mice treated with PBS alone and those treated with si-scramble ($P<0.05$). Moreover, the mice treated with si-*Stat3* showed markedly

Table 1 Tumour weights and sizes in different groups (mean±s.e.)

Group (n=8)	*Mean weight (g)*		*Mean tumour volume (cm^3)*
	Moush weight	*Tumour*	
Mock	24.7±0.9	6.8±1.7	4.5±0.5
HAP-si-scramble	25.1±2.2	5.2±1.3	3.4±0.3$^{\triangle}$
HAP-si-*Stat3*	25.3±1.4	2.7±1.4*	0.9±0.1*

*$P<0.01$ versus mock and HAP-si-scramble. $^{\triangle}P<0.05$ versus mock.

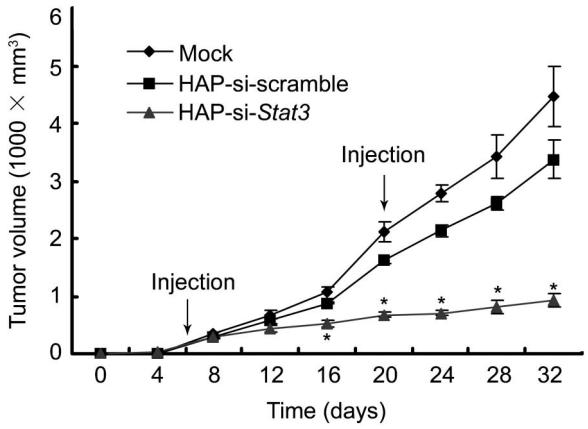

Figure 1 Growth curves of prostate tumours treated with si-*Stat3*. Mice were inoculated subcutaneously with cancer blocks (1.5 mm^3), and on day 5, these mice were divided into three groups and injected intratumourally with PBS, si-*Stat3* or si-scramble. This injection was repeated on day 20, and the tumour sizes were determined every 2 days. Data are presented as means±s.e. (n=8). *P<0.01 versus mock and si-scramble. PBS, phosphate-buffered saline; siRNA, small interfering RNA.

suppressed cancer growth when compared to the control mice (Figure 1; P<0.01).

Stat3 expression

To determine the ability of these plasmids to silence *Stat3* expression, RT-PCR and Western blot assay were used to analyse *Stat3* expression in tumours. The results indicated that the mRNA expression of *Stat3* and the protein expression of Stat3 and p-Stat3 were markedly reduced in tumours treated with si-*Stat3* compared with tumours treated with si-scramble or PBS alone (P<0.01; Figure 2).

The antitumour effects of si-*Stat3*

To determine the mechanism underlying the *in vivo* antitumour effects of si-*Stat3*, tumours were obtained and processed for immunohistochemistry and TUNEL assay. Immunohistochemical examination showed that the levels of Stat3, PCNA and CD34 were remarkably reduced by si-*Stat3* treatment when compared to the levels in the control group (Figure 3a–c). The proliferation index was 15.6±2.8% in the siRNA-*Stat3* group, which was significantly lower than in the control group (P<0.01, Table 2). The TUNEL assay showed that si-*Stat3*-treated cancers underwent massive apoptosis characterised by sparsely dispersed chromatin and necrotic tissues, as shown in Figure 3d and Table 2. The apoptosis index was 42.5±6.4% in the si-*Stat3* group, which was markedly higher than that in the control group (P<0.01). Hematoxylin and eosin staining showed that si-*Stat3*-treated tumours underwent high levels of apoptosis. There was no apparent invasion of the tumour into other tissues (data not shown). Si-*Stat3* treatment suppressed the expression of CD34 in tumours, thereby suppressing cancer growth. These findings suggest that $CaCl_2$-modified HAP can be used for the delivery of si-*Stat3* into tumours, exerting potent antitumour effects.

Expressions of *Stat3*-associated genes

Recent studies have indicated that constitutively active *Stat3* can induce the expression of several genes, including *Bcl-2* (which encodes an anti-apoptotic protein) and *cyclin D1* (which promotes cell

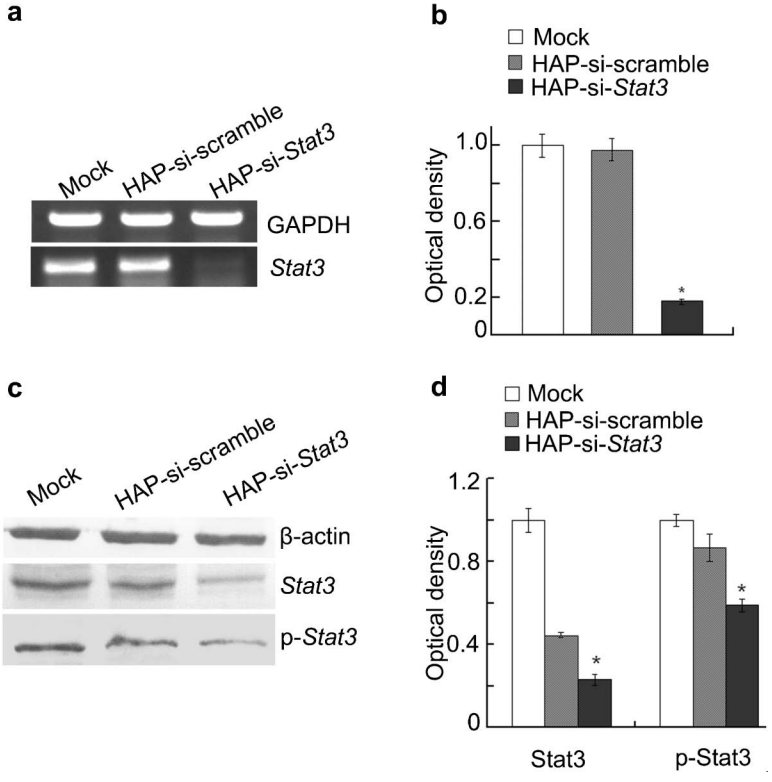

Figure 2 RT-PCR and Western blot assay of *Stat3* expression in prostate cancers. (**a**) Representative photographs from RT-PCR. (**b**) *Stat3* mRNA levels from three experiments. *P<0.01 versus mock and si-scramble. (**c**) Representative photographs from Western blot assay. (**d**) Protein expressions of Stat3 and p-Stat3 from three experiments. *P<0.01 versus mock and si-scramble. RT, reverse transcription; siRNA, small interfering RNA.

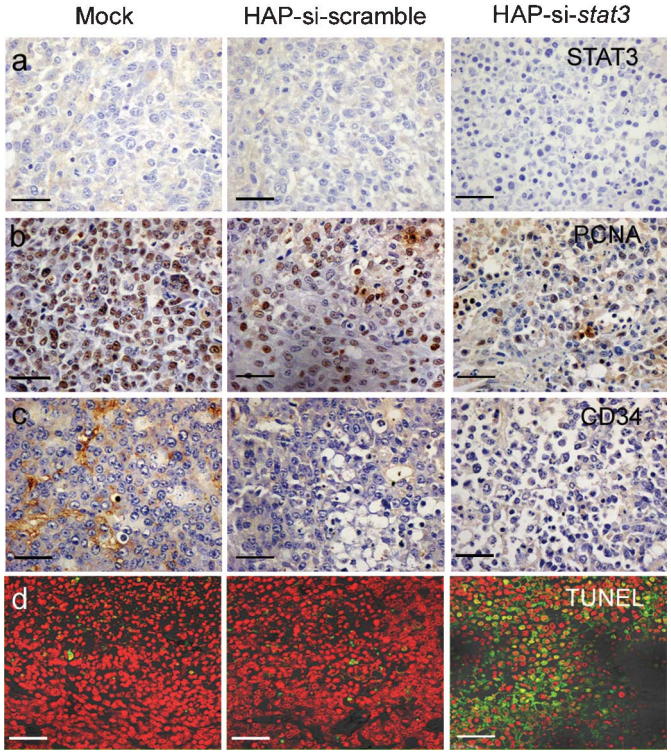

Figure 3 Immunohistochemistry and TUNEL assay. (**a**, **b**, **c**), immunohistochemical analyses of Stat3, PCNA and CD34 expression. Note a strong positive staining for Stat3, PCNA and CD34 in control group, in sharp contrast to those treated with si-*Stat3* (Scale Bar, 50 μm). **d**, TUNEL assay (Scale Bar, 33 μm). TUNEL-positive cells had green fluorescence.

division).[17] To determine the effects of si-*Stat3* treatment on the expression of *Stat3*-associated genes, Western blot assays were performed. The results showed that the levels of Bcl-2, VEGF and cyclin D1 proteins were dramatically downregulated in tumours, but Bax and Caspase3 levels were markedly elevated after si-*Stat3* treatment when compared with controls (Figure 4). These results imply that si-*Stat3* treatment interfered with the transcriptional activity of *Stat3*, subsequently reducing the expression of its downstream genes.

Table 2 The effects of *Stat3*-siRNA transfection on the proliferation and apoptosis of tumour cells

Group (n=8)	*PI (%) (mean±s.e.)*	*AI (%) (mean±s.e.)*
Mock	86.3±9.4	3.2±1.4
HAP-si-scramble	71.2±7.8	6.6±2.4
HAP-si-*Stat3*	15.6±2.8*	42.5±6.4*

Abbreviations: AI, apoptosis index; PI, proliferation index.
*$P<0.01$ versus mock and HAP-si-scramble.

DISCUSSION

Prostate cancer is a common disease in the elderly. In 2009, the new cases and deaths from prostate cancer in the United States were estimated to be 192 280 and 27 360, respectively.[18] In China, the incidence of prostate cancer has increased over time.[19] Surgery and radiotherapy with or without androgen deprivation therapy) are the most effective therapeutic strategies for prostate cancer. However, there is currently no effective treatment for patients with advanced prostate cancer at diagnosis and those who do not respond to primary curative attempts. It is imperative to develop novel, more effective strategies to treat prostate cancer. Because prostate cancer represents an accumulation of genetic mutations in cells that have gone awry, a novel approach against this cancer is gene therapy.[20]

Signal transducers and activators of transcription (STAT) proteins are a family of seven proteins (Stats 1, 2, 3, 4, 5a, 5b and 6) that mediate the transduction of extracellular signals to the transcription of target genes. Among the STATs, Stat3 is the most important, being closely linked to tumourigenesis.[21,22] Stat3 is a transcription factor and has been found in an activated state in numerous primary tumours.[23,24] Constitutive *Stat3* signalling represents one of the key molecular events in the multistep process leading to carcinogenesis. For these reasons, the *Stat3* signalling pathway can be used as a potential target in antitumour therapy.[25]

In our previous study, DNA vector-based *Stat3*-specific RNAi was used to block *Stat3* signalling.[12] However, the efficacy of siRNA-mediated interference depends on the efficient delivery of siRNA oligonucleotides. The challenge for siRNA delivery is even greater when the aim is to inhibit the *in vivo* expression of target genes. Delivering siRNA to animal tissues *in vivo* is a complicated process and involves

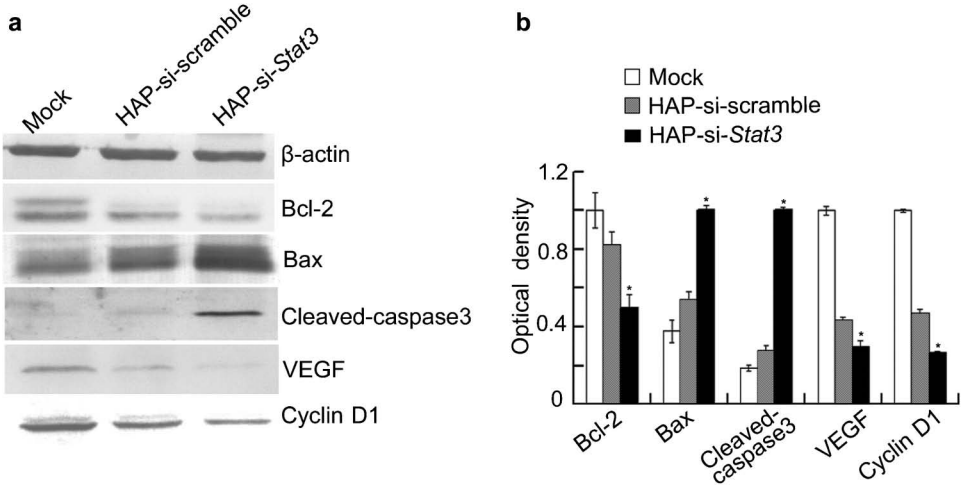

Figure 4 Western blot assay of *Stat3* downstream genes in prostate cancers transfected with si-*Stat3*. (**a**) Representative photographs from western blot assay. (**b**) Protein expression of Bcl-2, Bax, Caspase3, VEGF and cyclin D1 from three experiments. *$P<0.01$ versus mock and si-scramble. siRNA, small interfering RNA.

physical, chemical or biological approaches or a combination of them in some cases.[26] The major weaknesses limiting the wide application of most delivery systems are the potential for mutagenesis or oncogenesis, host immune responses and high cost.[27] Non-viral siRNA delivery to tissues does not elicit an immune response, has a great advantage in drug target validation and allows multiple administrations of siRNA, attributes that are crucial for the therapeutic application of siRNA. Sun *et al.*[11] successfully used HAP nanoparticles as a novel vector for inner ear gene therapy. Our results showed that $CaCl_2$-modified HAP can mediate the transfection of si-*Stat3* plasmids into mouse prostate cancer *in vivo*, resulting in the significant inhibition of cancer growth. Our results were consistent with reports that the transfection efficiency of HAP nanoparticles can reach as high as approximately 50–80% of that of liposome-mediated transfection.[10] In addition, our study showed that HAP alone could also exert antitumour effects: HAP carrying si-scramble could inhibit cancer growth compared to the control; this was consistent with the study of Zhu *et al.*, in which HAP alone could inhibit the *in vitro* proliferation of hepatocellular carcinoma cells.[10] Thus, the antitumour effects of HAP nanoparticles may be further enhanced when combined with *Stat3*-specific siRNA.

Our results showed that the levels of *Stat3* mRNA and protein were downregulated in cancer tissues after si-*Stat3* treatment, indicating that HAP can deliver *Stat3*-specific siRNA into cancer cells, resulting in the inhibition of *Stat3* expression. PCNA is a nuclear proliferation antigen, and its activation is closely related to cell proliferation.[28] Our immunohistochemical examination showed that PCNA-positive cells were decreased in the si-*Stat3* treatment group compared to controls, indicating that the downregulated expression of *PCNA* may be due to the suppression of *Stat3* expression by si-*Stat3* and may lead to inhibited proliferation of cancer cells. The TUNEL assay showed that apoptosis in the si-*Stat3* group was significantly increased. These findings reveal that the HAP carrying the si-*Stat3* can exert a potent antitumour effect *in vivo* by suppressing proliferation and promoting apoptosis of cancer cells. Furthermore, our results showed that the expression of pro-apoptotic factors including *Bax* and *Caspase3* was markedly upregulated in the si-*Stat3* group. However, anti-apoptotic factors such as *Bcl-2* and *cyclin D1* were reduced significantly. Studies have demonstrated that *Stat3* can upregulate the expression of several anti-apoptotic proteins, including Bcl-2 and Bcl-xL,[29] which are key components of mitochondrial apoptotic pathways. Therefore, si-*Stat3* transfection-induced apoptosis of cancer cells may be caused in part by the activation of mitochondrial apoptosis pathways.[30] Additionally, immunostaining assays revealed massive CD34 expression in cancers, an indicator of microvessel density in tissues. However, the expression of CD34 in tumours was significantly decreased after si-*Stat3* transfection, which was concurrent with the downregulation of VEGF, another gene downstream of *Stat3*, demonstrated by western blot assay. The reduced VEGF level resulting from *Stat3* knockdown was expected because VEGF expression has been shown to be upregulated by *Stat3*.[31] The downregulation of angiogenesis related factors (CD34 and VEGF) may lead to the suppression of cancer growth, resulting in reduced tumour size.

In conclusion, we have confirmed for the first time that HAP nanoparticles can be used as vectors in the *in vivo* delivery of plasmid-based siRNAs into cancers. The HAP nanoparticles carrying si-*Stat3* exhibited tumour-suppressive effects. These findings revealed that HAP may be used as an effective gene delivery tool. However, further modification of HAP is needed for high transfection efficiency and convenient clinical applications. Ultimately, we predict that research into *in vivo* siRNA delivery will translate into many clinically viable administration methods for siRNA-based therapeutics to treat various cancers.

AUTHOR CONTRIBUTIONS

ZWL and BFG carried out the study design and manuscript preparation. YL, XJL and XL carried out the molecular genetics studies and participated in data acquisition. LJZ and HY carried out the quality control of data and algorithms. LFG participated in the data analysis and interpretation. XJZ participated in the manuscript review. LZ and BXY carried out the study concepts, conceived the study, and helped to draft the manuscript. All authors read and approved the final manuscript.

COMPETING FINANCIAL INTERESTS

The authors declare that they have no competing financial interests.

ACKNOWLEDGMENTS

The authors would thank Mr Qiang-Lin Duan for English usage and paper revision.

This work was funded by the National Natural Science Foundation of China (No. 30801354, No. 30970791 and No. 30870921), the Fundamental Research Funds for the Central Universities of China (No. 200810012) and the Jilin Provincial Science & Technology Department, China (No. 20080154).

1 Sui G, Soohoo C, Affar el B, Gay F, Shi Y. A DNA vector-based RNAi technology to suppress gene expression in mammalian cells. *Proc Natl Acad Sci USA* 2002; **99**: 5515–20.
2 Wu MT, Wu RH, Hung CF, Cheng TL, Tsai WH. Simple and efficient DNA vector-based RNAi systems in mammalian cells. *Biochem Biophys Res Commun* 2005; **330**: 53–9.
3 Alshamsan A, Hamdy S, Samuel J, El-Kadi AO, Lavasanifar A *et al*. The induction of tumor apoptosis in B16 melanoma following STAT3 siRNA delivery with a lipid-substituted polyethylenimine. *Biomaterials* 2010; **31**: 1420–8.
4 Kumar GS, Girija EK, Thamizhavel A, Yokogawa Y, Kalkura SN. Synthesis and characterization of bioactive hydroxyapatite-calcite nanocomposite for biomedical applications. *J Colloid Interface Sci* 2010; **349**: 56–62.
5 Shi ZL, Huang X, Cai YR, Tang RK, Yang DS. Size effect of hydroxyapatite nanoparticles on proliferation and apoptosis of osteoblast-like cells. *Acta Biomaterialia* 2009; **5**: 338–45.
6 Levy-Nissenbaum E, Radovic-Moreno AF, Wang AZ, Langer R, Farokhzad OC. Nanotechnology and aptamers: applications in drug delivery. *Trends Biotechnol* 2008; **26**: 442–9.
7 Ye F, Guo HF, Zhang HJ, He XL. Polymeric micelle-templated synthesis of hydroxyapatite hollow nanoparticles for a drug delivery system. *Acta Biomaterialia* 2010; **6**: 2212–8.
8 McAllister K, Sazani P, Adam M, Cho MJ, Rubinstein M *et al*. Polymeric nanogels produced via inverse microemulsion polymerization as potential gene and antisense delivery agents. *J Am Chem Soc* 2002; **124**: 15198–207.
9 Hornez JC, Chai F, Monchau F, Blanchemain N, Descamps M *et al*. Biological and physico-chemical assessment of hydroxyapatite (HA) with different porosity. *Biomol Eng* 2007; **24**: 505–9.
10 Zhu SH, Zhou KC, Huang BY, Huang S, Liu F *et al*. Hydroxyapatite nanoparticles as a novel gene carrier. *Sheng Wu Yi Xue Gong Cheng Xue Za Zhi* 2005; **22**: 980–4. Chinese.
11 Sun H, Jiang M, Zhu SH. *In vitro* and *in vivo* studies on hydroxyapatite nanoparticles as a novel vector for inner ear gene therapy. *Zhonghua Er Bi Yan Hou Tou Jing Wai Ke Za Zhi* 2008; **43**: 51–7. Chinese.
12 Gao LF, Zhang L, Hu JD, Li F, Shao YT *et al*. Down-regulation of signal transducer and activator of transcription 3 expression using vector-based small interfering RNAs suppresses growth of human prostate tumor *in vivo*. *Clin Cancer Res* 2005; **11**: 6333–41.
13 Janik P, Briand P, Hartmann NR. The effect of estrone-progesterone treatment on cell proliferation kinetics of hormone-dependent GR mouse mammary tumors. *Cancer Res* 1975; **35**: 3698–704.
14 Zhang L, Gao LF, Li Y, Lin GM, Shao YT *et al*. Effects of plasmid-based Stat3-specific short hairpin RNA and GRIM-19 on PC-3M tumor cell growth. *Clin Cancer Res* 2008; **14**: 559–68.
15 Agarwala S, Kalil RE. Axotomy-induced neuronal death and reactive astrogliosis in the lateral geniculate nucleus following a lesion of the visual cortex in the rat. *Comp Neurol* 1998; **392**: 252–63.
16 Zhang L, Gao LF, Zhao LJ, Guo BF, Ji K *et al*. Intratumoral delivery and suppression of prostate tumor growth by attenuated *Salmonella enterica* serovar *typhimurium* carrying plasmid-based small interfering RNAs. *Cancer Res* 2007; **67**: 5859–64.

17 Alas S, Bonavida B. Rituximab inactivates signal transducer and activation of transcription 3 (STAT3) activity in B-non-Hodgkin's lymphoma through inhibition of the interleukin 10 autocrine/paracrine loop and results in down-regulation of Bcl-2 and sensitization to cytotoxic drugs. *Cancer Res* 2001; **61**: 5137–44.
18 Jemal A, Siegel R, Ward E, Hao Y, Xu J *et al*. Cancer statistics, 2009. *CA Cancer J Clin* 2009; **59**: 225–49.
19 Zhang L, Wu S, Guo LR, Zhao XJ. Diagnostic strategies and the incidence of prostate cancer: reasons for the low reported incidence of prostate cancer in China. *Asian J Androl* 2009; **11**: 9–13.
20 Zhang L, Zhao LJ, Zhao D, Lin GM, Guo BF *et al*. Inhibition of tumor growth and induction of apoptosis in prostate cancer cell lines by overexpression of tissue inhibitor of matrix metalloproteinase-3. *Cancer Gene Ther* 2010; **17**: 171–9.
21 Bromberg J, Wang TC. Inflammation and cancer: IL-6 and STAT3 complete the link. *Cancer Cell* 2009; **15**: 79–80.
22 Hirano T, Ishihara K, Hibi M. Roles of STAT3 in mediating the cell growth, differentiation and survival signals relayed through the IL-6 family of cytokine receptors. *Oncogene* 2000; **19**: 2548–56.
23 Al Zaid Siddiquee K, Turkson J. STAT3 as a target for inducing apoptosis in solidand hematological tumors. *Cell Res* 2008; **18**: 254–67.
24 Germain D, Frank DA. Targeting the cytoplasmic and nuclear functions of signal transducers and activators of transcription3 for cancer therapy. *Clin Cancer Res* 2007; **13**: 5665–9.
25 Lee SO, Lou W, Qureshi KM, Mehraein-Ghomi F, Trump DL *et al*. RNA interference targeting STAT3 inhibits growth and induces apoptosis of human prostate cancer cells. *Prostate* 2004; **60**: 303–9.
26 Lu PY, Xie F, Woodle MC. *In vivo* application of RNA interference: from functional genomics to therapeutics. *Adv Genet* 2005; **54**: 117–42.
27 Kim WJ, Kim SW. Efficient siRNA delivery with non-viral polymeric vehicles. *Pharm Res* 2009; **26**: 657–66.
28 Qin XG, Hua Z, Shuang W, Wang YH, Cui YD. Effects of matrine on HepG2 cell proliferation and expression of tumor relevant proteins *in vitro*. *Pharm Biol* 2010; **48**: 275–81.
29 Al Zaid Siddiquee K, Turkson J. STAT3 as a target for inducing apoptosis in solid and hematological tumors. *Cell Res* 2008; **18**: 254–67.
30 Niu G, Heller R, Catlett-Falcone R, Coppola D, Jaroszeski M *et al*. Gene therapy with dominant-negative Stat3 suppresses growth of the murine melanoma B16 tumor *in vivo*. *Cancer Res* 1999; **59**: 5059–63.
31 Chen Z, Han ZC. STAT3: a critical transcription activator in angiogenesis. *Med Res Rev* 2008; **28**: 185–200.